Gong *et al.*
Journal of Analytical Science and Technology (2023) 14:24
https://doi.org/10.1186/s40543-023-00390-5

Journal of Analytical Science and Technology

RESEARCH ARTICLE Open Access

A novel cysteine catalytic oxidation-based colorimetric approach for sensitive analysis of acute pancreatitis-related microRNA

Mingwei Gong[1], Guoyan Jiang[1], Yuan Rong[1], Zeping Yang[1], Dong She[1] and Chunhong Sun[1*]

Abstract

It is essential to establish simple, sensitive and accurate quantitative approaches for microRNAs (miRNAs) identification due to its crucial roles in a variety of physiological and pathological processes. Herein, we propose a novel RCA-based colorimetric method for sensitive and reliable miRNA analysis. In this approach, cyclization of the padlock sequence by miRNA-21 initiates the RCA to produce numerous G-rich sequences. The generated G-rich sequences fold to G-quadruplex DNAzyme that is capable of catalyzing cysteine to cystine which could mediate the gold nanoparticle-based color reaction, outputting results that can be observed directly by naked eyes. Based on this, the approach exhibits a wide detection range with a low limit of detection of 4 fM. In addition, the dual target recognition endows the method a greatly improved selectivity.

Keywords Rolling circle amplification, Gold nanoparticles (AuNPs), microRNAs (miRNAs), Cysteine

Introduction

MicroRNAs (miRNAs), a group of highly conserved single-stranded nucleotides that have evolved over time, are involved in a variety of physiological and pathological processes, including cell development, growth, and death (Diener et al. 2022; Mishra et al. 2016; Saliminejad et al. 2019). Recent research has demonstrated that altered miRNA expression has a role in the development of acute pancreatitis (AP) (Daoud et al. 2019; Ge et al. 2022; Wang et al. 2019). Indeed, it has been discovered that a number of miRNAs are dysregulated in a variety of cell types involved in AP and may serve as diagnostic biomarkers (Dey et al. 2021; Desai et al. 2021; Li et al. 2022). However, the characteristics of miRNAs, such as their short lengths, sensitivity to degradation, low quantity, and high sequence homology among family members, make it difficult to quantify miRNAs (Hua et al. 2022). Therefore, it is essential to establish simple, sensitive and accurate quantitative approaches for miRNA identification.

Northern blotting (Martinho and Lopez-Gomollon 2023; Zhang et al. 2022), quantitative reverse-transcription PCR (qRT-PCR) (Ban and Song 2022), and DNA microarray (Forte et al. 2022) remain the conventional methods that are commonly used to detect miRNAs in clinical practices. These methods have the advantages of high sensitivity and less samples requirement. But each approach has its own inherent drawbacks, such as low throughput, difficult probe design, and high cost (Jet et al. 2021). Strand-displacement amplification (SDA) (Wu et al. 2021), loop-mediated isothermal amplification (LAMP) (Gines et al. 2020), rolling circle amplification (RCA) (Song et al. 2022; Xu et al. 2019), and ligase chain reaction (LCR) (Yan et al. 2022a) have all demonstrated excellent sensitivity and selectivity in the detection of miRNAs in recent years. Among them, the RCA method has attracted abundant attention due to its simple experimental components, easy to operate characteristic, and

*Correspondence:
Chunhong Sun
chunhong21986@163.com
[1] Emergency Department, The Third Affiliated Hospital of Chongqing Medical University, No. 1 Shuanghu Branch Road, Yubei District, Chongqing 401120, China

high amplifying efficiency. Based on this, various RCA-based approaches have been proposed in recent years by integrating with different signal transducer. For example, Ruixuan Wang et al. developed a novel fluorescent method, termed RACE, for sensitive miRNA detection by combining the RCA with CRISPR-Cas9 system (Wang et al. 2020). By employing the RCA method to produce long single-strand DNA sequence (ssDNA) and CRISPR-Cas12a system for signal generation, a isothermal fluorescent assay was developed and was successfully applied for miRNA detection with limit of detection (LOD) in fM level. However, these methods require cumbersome equipment to read the fluorescent signals, which is a huge challenge to be applied in resource-limited scenes. To avoid this limitation, colorimetric approaches have been developed for miRNA detection. In contrast to fluorescent assays, the results provided by colorimetric approaches could be directly observed by naked-eyes, greatly simplifying the result readout procedures (Hosseinzadeh et al. 2020; Lan et al. 2019). However, the RCA-based colorimetric approaches have the instinct drawbacks, including (i) the sensitivity need further improvement; (ii) the false of RCA to distinguish mismatched bases may lead to false-positive results. Exonuclease, possessing the capability to specifically digest RNA sequences in DNA-RNA duplex (Yan et al. 2022b), inspired us to improve the RCA-based miRNA detection approaches.

Herein, we propose a novel RCA-based colorimetric method for sensitive and reliable miRNA analysis. In this approach, target sequence cyclizes the padlock sequence to induce the RCA, in which process numerous G-rich sequences are produced. The generated G-rich sequences fold to G-quadruplex DNAzyme that is capable of catalyzing cysteine to cystine. Cystine mediates the gold nanoparticle (AuNPs)-based color reaction, outputting results that can be observed directly by naked eyes. By the elaborate design, the specificity of RCA is greatly improved due the dual recognition, including the cyclization of padlock and exonuclease-I (Exo-I)/exonuclease-III (Exo-III)-based digestion of target sequence. In all, the proposed approach exhibits a high sensitivity and selectivity to target miRNA detection, which would be a robust tool for clinical diagnosis.

Results and discussion

The working principle of the established RCA-based colorimetric approach

The RCA-based colorimetric method's basic concept is schematically given in Fig. 1. The RCA-based colorimetric approach consists of two essential steps: the RCA reaction, also known as the target recognition-based ligation initiated RCA reaction, and the cysteine catalytic oxidation-based color reaction. There are three main steps in the RCA reaction. The first is the target sequence (with miRNA-21 as an example) perfectly hybridizes with

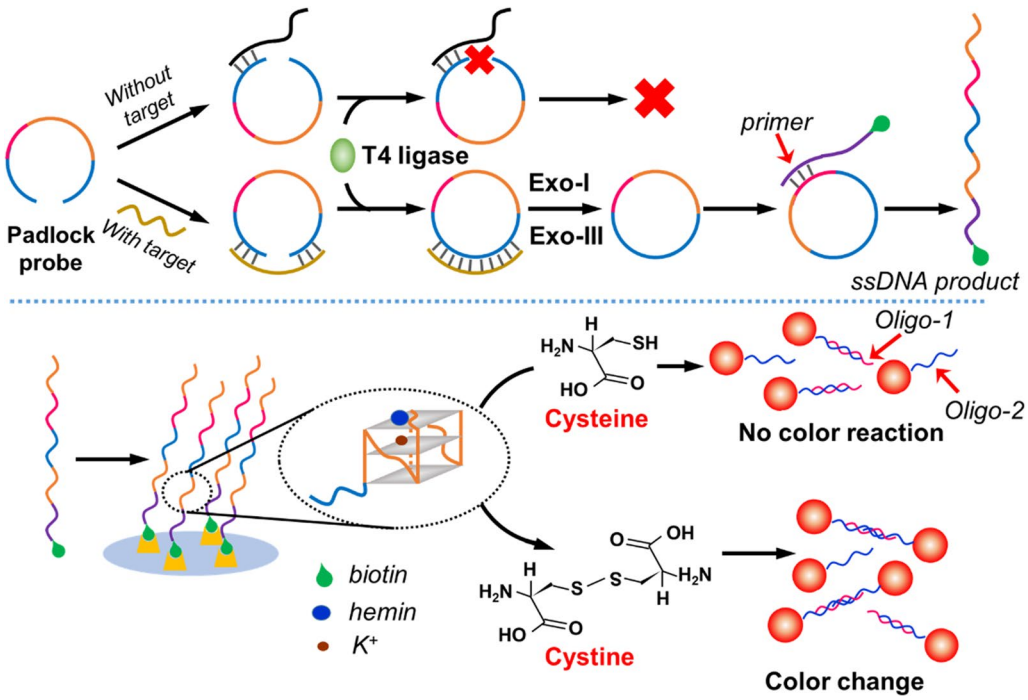

Fig. 1 The working mechanism of the established RCA-based approach

the 5' ends and 3' ends of linear padlock probes, followed by their ligation and circularization by DNA ligase, which prevents mismatches (the first recognition). Secondly, exonuclease I (Exo-I) is added to the above-ligation mixture to eliminate the unreacted padlock probes, and prevent self-ligation amplification that may cause strong background signals in the following RCA amplification. Exonuclease III (it has characteristics similar to RNaseH) is employed to destroy miRNA, which is the second target recognition. The biotin-labeled capture probes serve as primers to start the RCA reaction. The RCA products are lengthy single-stranded DNAs (ssDNAs) with tandem reduplicated G-rich regions that are biotin labeled at the 5′ terminus. This ssDNA product has been adhered to streptavidin-functionalized wells.

In the presence of hemin and K^+, these G-quadruplex sequences in ssDNA products act as a G-quadruplex-DNAzyme, accelerating the aerobic oxidation of cysteine to cystine and preventing Ag^+ from binding to the C•G∘C triad, a crucial component of triplex DNA. On the contrary, Ag^+ binds to C•G∘C triad that stabilizes the formation of triplex DNA between Oligo-1-modified AuNPs and Oligo-2, resulting in AuNP aggregation and a color change in the solution in a matter of minutes.

Proof-of-concept experiment of the RCA reaction and color reaction

In this approach, Exo-III is used to specifically remove the miRNA-21 in the cyclized padlock which constitute the second target recognition. To test the significant role of Exo-III in the RCA reaction, miRNA-21, which were labeled with FAM and BHQ at its two terminus, were utilized. In the synthesized miRNA-21, FAM maintained a close distance with BHQ, and the signal were quenched by the BHQ. Upon the addition of Exo-III, miRNA-21 sequences were digested, and FAM moiety was released to generate fluorescent signals (Fig. 2A). To investigate the synthesis of ssDNA product, a fluorescent assay was performed. In this assay, the biotin-labeled RCA product was fixed on the surface of streptavidin-functionalized wells. To characterize the repeated G-rich sections, FAM-labeled C-rich probes were incubated with ssDNA RCA products which were fixed on the well (Fig. 2B). The result in Fig. 2C showed that the recorded fluorescent signals were low when T4 DNA ligase, primer, and phi29 polymerase absent in the RCA reaction. Only when all essential components were existed, a greatly elevated signal could be observed, indicating the successful performance of RCA process and transcription of G-rich sections. The color reaction was demonstrated through recording the color change of the system.

The proof-of-concept experiment using UV–Vis absorption spectroscopy was carried out to examine the feasibility of this method. In the absence of target dsDNA, a surface plasmon resonance absorption peak for scattered Oligo-1-modified AuNPs at 525 nm was observed (Fig. 2D), and the solution color remained red (inset in Fig. 2D, image a). The absence of target dsDNA prevented AuNP assembly, which was attributed to Ag–S formation between Ag^+ and cysteine, which prevented triplex DNA creation between Oligo-1 on AuNPs and Oligo-2. On the contrary, when target dsDNA was added, the absorbance at 525 nm dropped dramatically, accompanied by a color shift from red to blue.

Optimization of experimental conditions

The RCA reaction and a color reaction based on cysteine catalytic oxidation were used to construct the colorimetric biosensor for miRNA-21 detection. Therefore, it was necessary to optimize the relevant factors that could impact the assay's sensitivity, including the enzyme concentrations (T4 ligase, phi29 polymerase, Exo-I and Exo-III), K^+, hemin, cysteine, and Ag^+. The ratio of absorbance at 600 and 525 nm (A600/A525) was used to indicate the aggregation of AuNPs because the absorbance of 525 nm steadily shifted and decreased along with the increase at 600 nm in the presence of target dsDNA. This method has the advantage of eliminating errors caused by variations in AuNPs concentration. From Fig. 3A, A600/A525 increased with the concentration of phi29 polymerase ranged from 0 to 1.5 U/L, reaching a plateau with more concentrations of phi29 enzyme. 1.5 U/L of the phi29 polymerase was then employed in following experiments. Meanwhile, 1 U/L T4 DNA ligase, 1 U/L Exo-I, and 0.5 U/L Exo-III were also determined to be used in the following experiments. In Fig. 3B, C, the effects of hemin and Ag^+ were also examined. A600/A525 increased as hemin and Ag^+ concentrations rose, plateauing at 2 μM and 15.0 μM, respectively. As a result, 2 μM and 60.0 mM were chosen as the ideal concentrations for Ag^+ and hemin, respectively. The best K^+ concentration was chosen to be 60.0 mM after further investigation revealed that A600/A525 increased as K^+ concentration increased and reached a plateau at this level (Fig. 3C). The same method was also used to optimize other variables, including 16.0 M of cysteine (Fig. 3D).

Analytical performance of the RCA-based colorimetric approach

After optimizing the experimental parameters, the performance of the approach was investigated. The RCA-based colorimetric method could clearly demonstrate color changes and absorbance responses to various concentrations of miRNA-21, as shown in Fig. 4A. Over an 6-order-of-magnitude range from 10 fM to 1 nM, a linear association between A600/A525 values and logarithmic

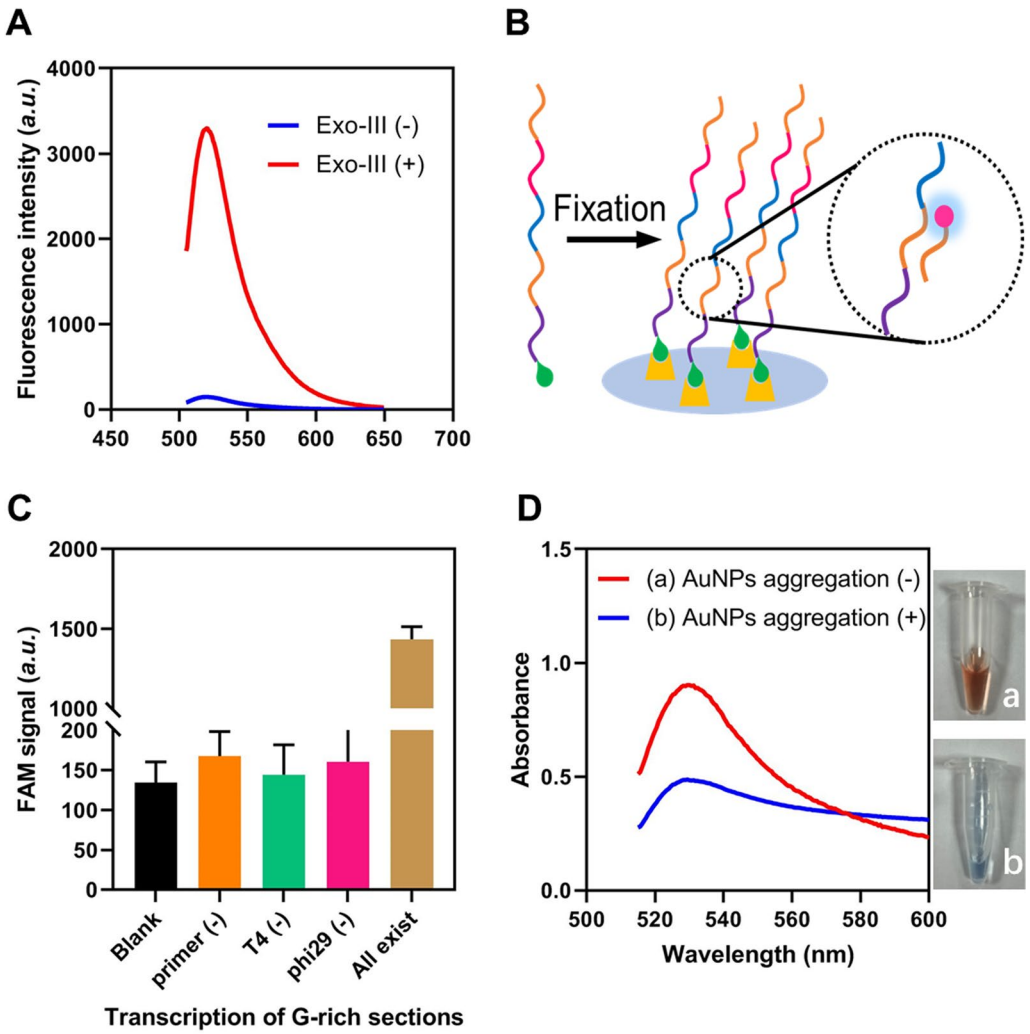

Fig. 2 Feasibility of the RCA reaction and color reaction. **A** fluorescence spectrum of the FAM-labeled miRNA when exonuclease-III (Exo-III) existed or not. **B** Schematic illustration of the fluorescent assay to test the RCA product. **C** FAM signals of the RCA product when primer, T4 DNA ligase, and phi29 enzyme were existed in the system or not. **D** Absorbance of the AuNPs before and after aggregation. Inserted is the color change of AuNPs, a, before aggregation; b, after aggregation

concentrations of miRNA-21 was found. The limit of detection was calculated to be 4 fM using the linear correlation equation $Y = 0.1108^{*}\lg C + 0.1101$ (Fig. 4B). The sensing platform provides highly specificity in addition to sensitivity. The miRNA-21 and its one-base (m1), two-base (m2), and three-base (m3) variants of the same concentration (100 pM) resulted in significantly different A600/A525 values. The A600/A525 value achieved using 1 nM of m1 was equivalent to that obtained using 10 fM of miRNA-21, while the value obtained using 1 nM of m2 was equivalent to that obtained using blank. There was no discernible A600/A525 value provided for the noncognate let-7a (Fig. 4C). To verify the applicability of the method to clinical sample analysis, artificial serum samples were created by diluting target miRNA into a commercially available serum solution. The correlation coefficient of 0.9943 in Additional file 1: Fig. S1 between the detection results and the initial quantities of miRNA-21 indicates that the method is capable of detecting miRNAs from clinical samples.

Conclusion

Here, we present a quick and accurate colorimetric approach that relies on the aggregation of DNA-modified AuNPs brought on by G-quadruplex DNAzyme to detect miRNAs associated with acute pancreatitis. This platform has a solid linear relationship with the logarithmic concentrations of miRNA-21, possessing a record detection

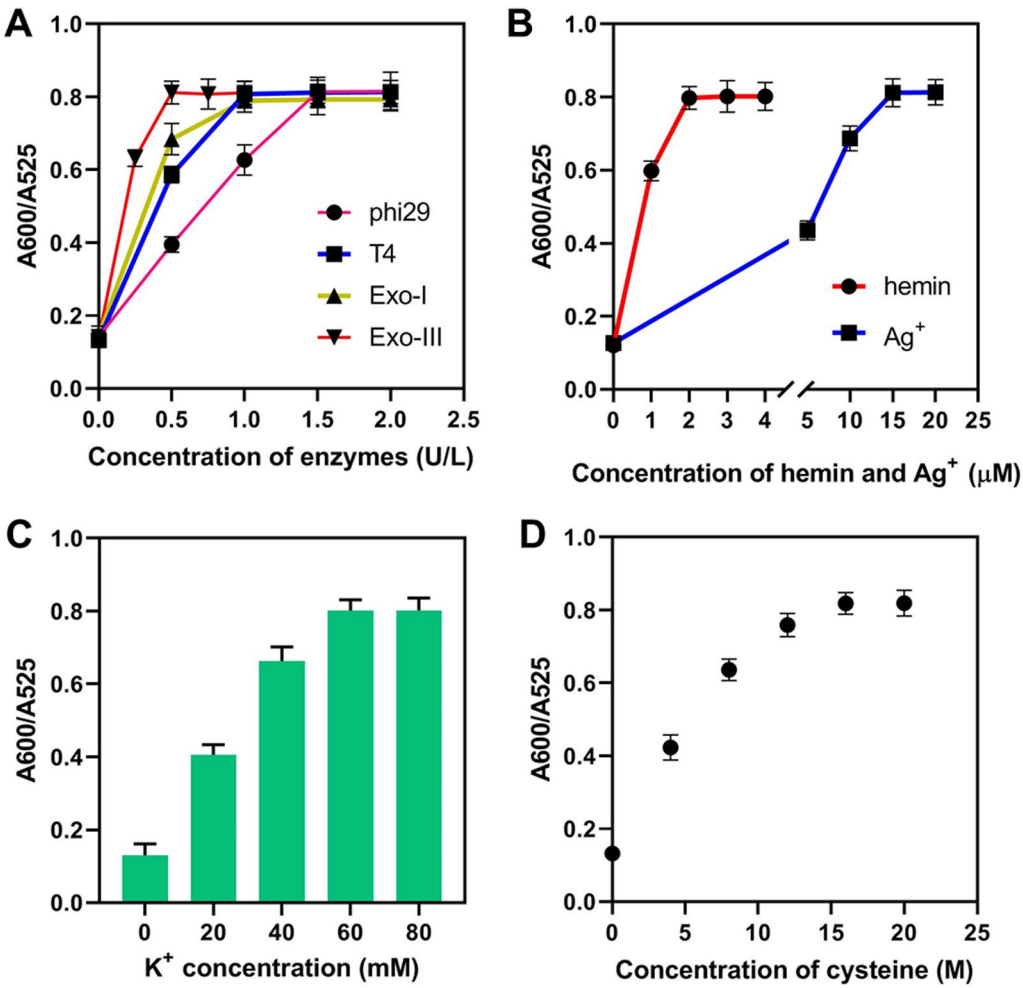

Fig. 3 Optimization of experimental parameters. A600/A525 ratio of the approach with different concentrations of enzymes (**A**), hemin and Ag^+ (**B**), K^+ (**C**), cysteine (**D**)

limit of 4 fM using miRNA-21 as a model analyte. Additionally, the addition of RCA product changed the color of DNA-modified AuNPs probes into blue within 10 min, enabling quick and clear identification of miRNA-21. With respect to reaction time, sensitivity, and selectivity, this colorimetric platform exhibits potential for sensing miRNAs associated with acute pancreatitis.

Experimental section

Materials and apparatus

Additional file 1: Table S1 displays these sequences that are used in this approach, such as the probes and biotin-labeled primer sequence. All oligonucleotides were purchased from Sangon Biotech Co., Ltd. (Shanghai, China). We bought phi29 DNA polymerase, dNTPs, T4 DNA ligase, Exonuclease I, and Exonuclease III from New England Biolabs Co., Ltd. (Beijing, China). Streptavidin, 96-well plates, biotin-secondary antibody, and AuNPs were obtained from Thermo scientific Co., Ltd (Beijing, China). All other chemicals were in analytical grade.

Preparation of plates

The 96-well plates were first filled with biotin-secondary antibody (0.25 g well1), which was then incubated for 3 h at 37 °C. After removing extra biotin-secondary antibody, washing buffer was used to wash the 96-well plates. To avoid non-specific adsorption, 200 μL of 0.5% skim milk (w/v) was added to the 96-well plates. The 96-well plates were washed with washing buffer after being incubated at 37 °C for 1 h. The 96-well plates were then filled with 1 g of streptavidin and incubated at 37 °C for 1 h. The 96-well plates were then washed with washing buffer while being kept at 4 °C after any extra reagent was decanted.

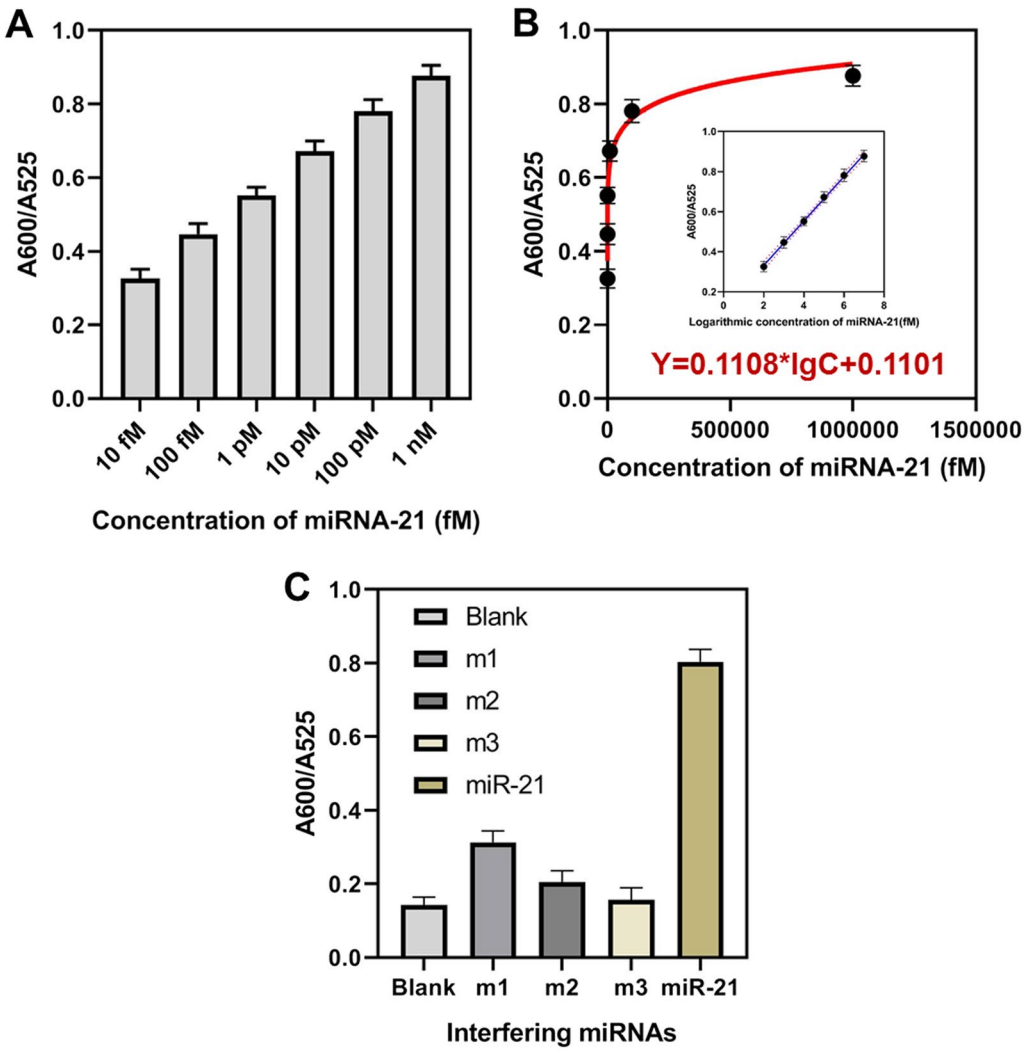

Fig. 4 Detection performance of the established approach. **A** A600/A525 values of the approach when detecting different concentrations of miRNA-21. **B** Correlation between the calculated A600/A525 values and the concentrations of miRNA-21. **C** A600/A525 values of the approach when miRNA-21 and mismatched miRNAs

RCA reaction

The target sequence and the linear padlock probes were denatured at 95 °C for 5 min before being gradually cooled to room temperature. 1 U of T4 DNA ligase was then added after the mixture had been incubated at 50 °C for 60 min. For 60 min, the ligation mixture was incubated at 30 °C. Then, each reaction received 1 L of an exonuclease mixture containing 1 U of exonuclease I and 0.5 U of exonuclease III. The mixed solution underwent a 1-h incubation period at 37 °C, followed by a 15-min inactivation period at 95 °C. The above-mentioned products were then introduced to RCA reaction system along with 10 μL phi 29 DNA polymerase buffer, 1 mM biotin-labeled primer, 1.5 U phi29 DNA polymerase, 1 mM dNTPs for 90 min and inactivated at 65 °C for 10 min. For additional examination, the end results—long, reduplicated single-strand DNA sequences—that had been biotin labeled at the 5′ terminus were employed.

Color reaction

The RCA product was heated for 10 min at 90 °C before being cooled off gradually to room temperature. After the appropriate amount of potassium acetate (KOAc) was added to the DNA solution at room temperature, the G-quadruplex structure was formed. In order to stabilize the hemin/G-quadruplex-based DNAzyme in Tris-OAc buffer (10 mM, pH 8.0), the G-quadruplex-based DNAzyme was incubated with hemin at room temperature for approximately 1 h. Then, the mixture was incubated with mild cysteine for 30 min. Afterward, the mixture were incubated for 10 min with 3.7 nM Oligo-1 modified

AuNPs and a specific amount of Oligo-2. Using a UV–Vis spectrophotometer, the color absorption spectrum was estimated.

Supplementary Information

The online version contains supplementary material available at https://doi.org/10.1186/s40543-023-00390-5.

Additional file 1. Fig. S1. The correlation between the calculated miRNA-21 concentration by the method and the initial concentration of miRNA-21. **Table S1**. Sequences of oligonucleotides used in this research.

Acknowledgements
The authors thank financial and technical support from The Third Affiliated Hospital of Chongqing Medical University.

Author contributions
C. S. is the supervisor of the team in all research steps including designing, data analysis and manuscript writing. M. G., as the first author, has the main role for experimental data collection, data gathering, preparation of results, and data analysis. G. J., Y. R., Z. Y., and D. S. assist the data analysis.

Funding
No fund available.

Availability of data and materials
Almost all details of experimental data are presented in the article or additional file.

Declarations

Ethics approval and consent to participate
The manuscript does not contain clinical or trial studies on patients, humans, or animals.

Competing interests
The authors declare that they have no competing interests.

Received: 24 April 2023 Accepted: 8 June 2023
Published online: 19 June 2023

References

Ban E, Song EJ. Considerations and Suggestions for the Reliable Analysis of miRNA in Plasma Using qRT-PCR. Genes (Basel), 2022;13.
Daoud AZ, Mulholland EJ, Cole G, McCarthy HO. MicroRNAs in pancreatic cancer: biomarkers, prognostic, and therapeutic modulators. BMC Cancer. 2019;19:1130.
Desai CS, Khan A, Bellio MA, Willis ML, Mahung C, Ma X, Baldwin X, Williams BM, Baron TH, Coleman LG, Wallet SM, Maile R. Characterization of extracellular vesicle miRNA identified in peripheral blood of chronic pancreatitis patients. Mol Cell Biochem. 2021;476:4331–41.
Dey S, Udari LM, RiveraHernandez P, Kwon JJ, Willis B, Easler JJ, Fogel EL, Pandol S, Kota J. Loss of miR-29a/b1 promotes inflammation and fibrosis in acute pancreatitis. JCI Insight. 2021; 6.
Diener C, Keller A, Meese E. Emerging concepts of miRNA therapeutics: from cells to clinic. Trends Genet. 2022;38:613–26.
Forte G, Ventimiglia G, Pesaturo M, Petralia S. A highly sensitive PNA-microarray system for miRNA122 recognition. Biotechnol J. 2022;17:e2100587.
Ge W, Goga A, He Y, Silva PN, Hirt CK, Herrmanns K, Guccini I, Godbersen S, Schwank G, Stoffel M. miR-802 suppresses acinar-to-ductal reprogramming during early pancreatitis and pancreatic carcinogenesis. Gastroenterology. 2022;162:269–84.
Gines G, Menezes R, Xiao W, Rondelez Y, Taly V. Emerging isothermal amplification technologies for microRNA biosensing: applications to liquid biopsies. Mol Aspects Med. 2020;72:100832.
Hosseinzadeh E, Ravan H, Mohammadi A, Pourghadamyari H. Colorimetric detection of miRNA-21 by DNAzyme-coupled branched DNA constructs. Talanta. 2020;216:120913.
Hua X, Fan J, Yang L, Wang J, Wen Y, Su L, Zhang X. Rapid detection of miRNA via development of consecutive adenines (polyA)-based electrochemical biosensors. Biosens Bioelectron. 2022;198:113830.
Jet T, Gines G, Rondelez Y, Taly V. Advances in multiplexed techniques for the detection and quantification of microRNAs. Chem Soc Rev. 2021;50:4141–61.
Lan L, Wang RL, Liu L, Cheng L. A label-free colorimetric detection of microRNA via G-quadruplex-based signal quenching strategy. Anal Chim Acta. 2019;1079:207–11.
Li X, Qin H, Anwar A, Zhang X, Yu F, Tan Z, Tang Z. Molecular mechanism analysis of m6A modification-related lncRNA-miRNA-mRNA network in regulating autophagy in acute pancreatitis. Islets. 2022;14:184–99.
Martinho C, Lopez-Gomollon S. Detection of microRNAs by northern blot. Methods Mol Biol. 2023;2630:47–66.
Mishra S, Yadav T, Rani V. Exploring miRNA based approaches in cancer diagnostics and therapeutics. Crit Rev Oncol Hematol. 2016;98:12–23.
Saliminejad K, Khorram Khorshid HR, Soleymani Fard S, Ghaffari SH. An overview of microRNAs: biology, functions, therapeutics, and analysis methods. J Cell Physiol. 2019; 234:5451–65.
Song J, Ju Y, Kim S, Kim H, Park HG. Palindromic hyperbranched rolling circle amplification enabling ultrasensitive microRNA detection. Chem Commun (cambridge). 2022;58:6518–21.
Wang W, Lou W, Ding B, Yang B, Lu H, Kong Q, Fan W. A novel mRNA-miRNA-lncRNA competing endogenous RNA triple sub-network associated with prognosis of pancreatic cancer. Aging (albany NY). 2019;11:2610–27.
Wang R, Zhao X, Chen X, Qiu X, Qing G, Zhang H, Zhang L, Hu X, He Z, Zhong D, Wang Y, Luo Y. Rolling circular amplification (RCA)-assisted CRISPR/Cas9 cleavage (RACE) for highly specific detection of multiple extracellular vesicle MicroRNAs. Anal Chem. 2020;92:2176–85.
Wu Y, Fu C, Shi W, Chen J. Recent advances in catalytic hairpin assembly signal amplification-based sensing strategies for microRNA detection. Talanta. 2021;235:122735.
Xu M, Ye J, Yang D, Abdullah Al-Maskri AA, Hu H, Jung C, Cai S, Zeng S. Ultrasensitive detection of miRNA via one-step rolling circle-quantitative PCR (RC-qPCR). Anal Chim Acta. 2019;1077: 208–15.
Yan X, Zhang J, Jiang Q, Jiao D, Cheng Y. Integration of the ligase chain reaction with the CRISPR-Cas12a system for homogeneous, ultrasensitive, and visual detection of microRNA. Anal Chem. 2022a;94:4119–25.
Yan T, Zhang S, Yang Y, Li Y, Xu LP. Biomineralization-inspired magnetic nanoflowers for sensitive miRNA detection based on exonuclease-assisted target recycling amplification. Mikrochim Acta. 2022b;189:260.
Zhang L, Su W, Liu S, Huang C, Ghalandari B, Divsalar A, Ding X. Recent progresses in electrochemical DNA biosensors for MicroRNA detection. Phenomics. 2022;2:18–32.

Publisher's Note